HOSTED BY

ELSEVIER

CrossMark

Available online at www.sciencedirect.com

ScienceDirect

Progress in Natural Science: Materials International 25 (2015) 419–424

Progress in Natural Science Materials International

www.elsevier.com/locate/pnsmi
www.sciencedirect.com

Original Research

Structural and dielectric properties of doped ferrite nanomaterials suitable for microwave and biomedical applications

Imran Sadiq[a,*], Shahzad Naseem[a], Muhammad Naeem Ashiq[b], M.A. Khan[c], Shanawer Niaz[d], M.U. Rana[a]

[a]Centre of Excellence in Solid State Physics, University of the Punjab, Lahore, Pakistan
[b]Institute of Chemical Sciences, Bahauddin Zakariya University, Multan 60800, Pakistan
[c]Department of Physics, BUITEMS, Quetta, Pakistan
[d]Department of Physics, University of Sargodha, Sargodha, Pakistan

Received 14 May 2015; accepted 31 July 2015
Available online 31 October 2015

Abstract

The sol–gel auto-combustion method was adopted to synthesize nanomaterials of single-phase X-type hexagonal ferrites with the composition of $Sr_{2-x}Gd_xNi_2Fe_{28-y}Cd_yO_{46}$ ($x=0.00$, 0.02, 0.04, 0.06, 0.08, 0.10 and $y=0$, 0.1, 0.2, 0.3, 0.4, 0.5). The structural properties were carried out by XRD analysis and the lattice parameters show variation with the doping of Gd–Cd. The average particle size measured by TEM was in the range of 8–10 nm which is beneficial in obtaining suitable signal-to-noise ratio in recording media and biomedical applications. The room temperature resistivity enhanced with the increase of the dopant concentration. The increase in resistivity indicates that the synthesized materials can be considered good for the formation of the multilayer chip inductors (MLCIs) as well as for the reduction of eddy current losses. The dielectric constant decreased with the increase in the frequency which is the general reported trend of the hexagonal ferrites and can be explained on the basis of Koop's theory and Maxwell–Wagner polarization-model. The abnormal dielectric behavior indicates the formation of small polarons in the material. The maximum value of tangent loss at low frequencies reflects the application of these materials in medium frequency devices (MF).

Keywords: Sol–gel; Nanocrystalline materials; Thermal properties; Electrical properties; Dielectric properties

1. Introduction

With the rapid development of modern communication technique and electronic devices in recent years, the electromagnetic and microwave radiation pollutions are becoming a serious problem. As a result, more and more researches are focusing on developing antiradiation materials and microwave absorbing materials [1–5]. Magnetoplumbite hexaferrites are suitable for electromagnetic interference suppression and radar absorbent materials due to their strong magnetic losses at gigahertz frequency [6]. For the hexagonal structure, there are six possible different types namely M, W, X, Y, Z and U. All the complex hexaferrites are structurally different with respect to the combinations of S ($2MFe_2O_4$), R (Ba/Sr Fe_6O_{11}) and/or T ($(Ba/Sr)_2$ Fe_8O_{14}) blocks while the Gibbs free energies of their formation are similar, and the thermodynamic conditions for their formation are also similar. Therefore, a local inhomogeneity and/or non-stoichiometry in the reaction mixtures with the stoichiometry of a particular hexaferrite (e.g.,W-hexaferrite=(RSS)$_2$) can result in the formation of another hexaferrite with a slightly different combination of structural blocks (e.g., X-hexaferrite=(RS)2S) [7–8]. Among all the hexagonal ferrites, the X-type hexaferrites with low coercivity and high saturation magnetization can be considered good for microwave absorption properties and the preparation of single phase X-type hexagonal ferrite requires very high temperature which is the challenging task [14]. Furthermore, the rare earth

*Corresponding author. Tel.: +92 42 99231136.
E-mail address: khanphysics@yahoo.com (I. Sadiq).

http://dx.doi.org/10.1016/j.pnsc.2015.09.011

elements substituted materials exhibit a variety of effects originating from the coupling between two spin subsystems. As the transition elements are very less anisotropic than the rare earth elements, the orientations of the hexagonal ferrites can be controlled with the substitution of rare earth elements in pure ferrites, which affects the magnetic, optical and elastic properties significantly [9–10].

Many researchers have synthesized and characterized the rare earth elements doped nanoferrites. Ashiq et al. [8] have reported the structural, electrical and magnetic properties of Gd–Sn substituted $Sr_{1-x}Gd_xFe_{12-y}Sn_yO_{19}$ (where $x=0.00$, 0.025, 0.05, 0.075, 0.1 and $y=0.00$, 0.25, 0.5, 0.75, 1) prepared by the sol–gel combustion method. The average crystallite size lies in the range of 19–42 nm. DC electrical resistivity shows the transition of metal to semiconductor with temperature, and the magnetic properties of the samples decreased with additives. The citrate-precursor method was adopted to synthesize the rare earth element La^{3+} substituted $Sr_{1-x}La_xFe_{12}O_{19}$ ($x=0$, 0.08, 0.13, 0.18) M-type hexaferrites by Want et al. [11]. The dielectric, conducting and impedance properties were measured as a function of frequency and additive concentration in the frequency ranges of 20 Hz to 3 MHz. The decrease in saturation magnetization and increase in coercivity were observed with the increase of La^{3+} concentration. However, the structural, electrical and dielectric properties of Gd–Cd doped X-type hexagonal ferrites have seldom been reported.

In the present work, an attempt has been made to synthesize the single phase $Sr_{2-x}Gd_xNi_2Fe_{28-y}Cd_yO_{46}$ ($x=0.00$, 0.02, 0.04, 0.06, 0.08, 0.10 and $y=0$, 0.1, 0.2, 0.3, 0.4, 0.5) X-type hexagonal nanoferrites by using the sol–gel method, and the effect of Gd–Cd substitution on the structural, electrical and dielectric properties of X-type hexagonal nanoferrites has been investigated.

2. Experimental procedure

The polycrystalline X-type hexaferrites and its derivatives with composition of $Sr_{2-x}Gd_xNi_2Fe_{28-y}Cd_yO_{46}$ ($x=0.00$, 0.02, 0.04, 0.06, 0.08, 0.10 and $y=0$, 0.1, 0.2, 0.3, 0.4, 0.5) were prepared by the sol–gel method. The stoichiometric ratios of raw materials $Sr(No_3)_2$, $Cd(No_3)_2$, $NiCl_2\cdot 6H_2O$, Gd_2O_3, Iron nitrate, Citric Acid were mixed in deionized water. The gel was attained by stirring the solution at 80 °C. The gel was burnt at 400 °C for 1 h and finally sintered at 1250 °C for 6 h to attain the required phase. The powder was then pressed into pellets at a pressure of ~30 KN using Paul-Otto Weber hydraulic press by using Polyvinyl alcohol as binder.

The thermal analysis to conform the temperature at which required phase can be obtained was carried out by the Mettler Toledo TGA/DSC 1 STAR^e system equipped with Nitrogen gas. The crystalline phase after heat treatment was identified by using a Schimadzu X-Ray diffractometer equipped with Cu-Kα radiations ($\lambda=1.5406$ Å). The particle morphology was examined by JEOL JSM-6500F field emission scanning electron microscopy and TECNAI F20 Phillips High Resolution Transmission Electron Microscopy. The electrical properties were measured by a two probe method, using source meter

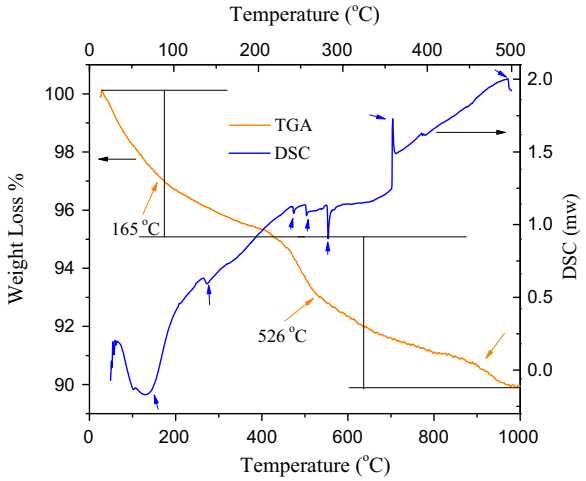

Fig. 1. (a) Thermogravimetric analysis curve for the precursor pre-sintered at 400 °C and (b) differential scanning calorimetric curve of the as synthesized precursor.

model Keithly 2400. The dielectric properties have been measured by LCR Meter. The dielectric constant was measured by using formula $\varepsilon=Cd/A\varepsilon_o$ where C is the capacitance in Farad, ε_o is the permittivity of free space (8.85×10^{-12} F m^{-1}), A is the area of cross section of flat surface of the pellet and d is the pellet thickness.

3. Results and discussion

3.1. Thermal analysis

Fig. 1(a) shows the thermogravimetric analysis of pre-sintered precursor at 400 °C for 1 h. The thermogravimetric curve can be subdivided into two endothermic peaks and an exothermic peak in the end. The endothermic peak in the temperature ranges of 120–235 °C shows the weight loss which can be attributed to the dehydration of absorbed water by the pre-sintered precursor. For the second endothermic peak, a sharp weight loss can be observed in the temperature range of 490–565 °C, which shows the oxidation of organic impurities and formation of metal oxides. The broad exothermic peak in the end of the curve shows the formation of hexagonal structure [12]. The differential scanning calorimetric curve indicates that the sample experiences the strong endothermic and exothermic changes, which may be attributed to the dehydration of water, decomposition of organic compounds and formation of metal oxides.

3.2. Structural properties

XRD patterns of X-type hexagonal ferrites sintered at 1250 °C for 6 h are shown in Fig. 2. Hexagonal single phase can be confirmed from the XRD patterns. Lattice parameters a (Å) and c (Å) were calculated by using formula;

$$\frac{1}{d_{hkl}^2}=\frac{4\left(h^2+hk+k^2\right)}{3a^2}+\frac{l^2}{c^2} \quad (1)$$